第23卷 第6期 高能物理与核物理 Vol.23, No.6
1999 年6月 HIGH ENERGY PHYSICS AND NUCLEAR PHYSICS June, 1999

Infra-red Renormalisation Group Calculation of the $O(N)$ Model in the Broken Phase

Liu Chuan

(*Department of Physics, Peking University, Beijing* 100871)

Abstract The infra-red renormalization properties of the $O(N)$ model is studied to two loops. The calculation is done within a mass dependent renormalization scheme. The mass-dependent one-loop renormalization group coefficients are obtained and the two-loop coefficients are calculated in the infrared limit. We observe cancellations within the framework of field theory which make the two-loop beta-function coincide with the one-loop beta-function in the infra-red limit.

Key words infra-red renormalisation group, effective Lagrangian, $O(N)$ model, broken symmetry

1 Introduction

The $O(N)$ model in the broken phase has Goldstone particles due to the spontaneous breaking of the $O(N)$ symmetry to $O(N\text{-}1)$. It has been understood that these Goldstone particles dominate the low energy behavior of the theory. At $N=4$, this model is the same as the Higgs sector in the minimal Standard Model. It also shares the similar symmetry breaking pattern as that of low energy QCD.

When studying the low energy limit of the theory, the effective Lagrangian approach has been commonly used. A well-known successful example of the effective Lagrangian goes back to low energy QCD phenomenology where Chiral Perturbation theory was applied. For a review of this, see Ref. [1] and references therein. Using the symmetry of the theory, Chiral Perturbation theory can make all low energy predictions in terms of a few phenomenological coupling constants. These low energy predictions should agree with those obtained with a direct field theoretical calculation in the low energy regime. At higher energies, roughly around the rho meson mass in QCD, unitarity is violated in Chiral Perturbation theory and effective Lagrangian as a derivative expansion looses its meaning. It is therefore desirable to have a direct comparison between Chiral Perturbation theory and the direct field theoretical calculation. However, this is not feasible in QCD due to the nonperturbative feature of the theory at low energies.

In the case of the $O(N)$ model (also known as the linear sigma model), it is believed that, up until the scale of the mass of the sigma particle, all low energy Green functions of the theory can be calculated using the effective Lagrangian approach. Within the framework of field theory, unlike QCD, $O(N)$ model is perturbative in the low energy

Received 4 January 1999

regime. Therefore, it is possible and interesting to compute the low energy quantities using both approaches. There is one subtlety when performing the calculation within the field theoretical approach, namely, the potential infra-red divergences in the theory due to Goldstone modes. In this letter, we compute the full mass-dependent renormalization group coefficients to one-loop and the leading infra-red behavior of the renormalization coefficients to two-loop within the field theoretical approach. In section 2, the Lagrangian for the $O(N)$ model in the broken phase is given and three mass-dependent renormalization conditions are introduced. The full mass-dependent renormalization coefficients are then obtained to one-loop. The physical significance of the result is also discussed. In Section 3, we calculate the two-loop diagrams that contribute to the two-loop renormalization coefficients in the infra-red limit. It is shown that these dominant two-loop diagrams cancel each other yielding a vanishing result to the renormalization group coefficients in the infra-red limit. The significance of this cancellation and the comparison with the effective Lagrangian approach is also addressed.

2 The $O(N)$ Model in the Broken Phase

We start with the standard Lagrangian for the $O(N)$ model in $D\equiv 2\omega$ space-time dimensions,

$$L=\frac{1}{2}\partial_\mu\phi^a\partial_\mu\phi^a-\frac{\mu^2}{2}\phi^a\phi^a+\frac{\lambda\Lambda^{2\varepsilon}}{4!}(\phi^a\phi^a)^2+\delta L, \tag{1}$$

$$\delta L=\frac{\delta Z}{2}\partial_\mu\phi^a\partial_\mu\phi^a-\frac{\delta\mu^2}{2}\phi^a\phi^a+\frac{\delta\lambda\Lambda^{2\varepsilon}}{4!}(\phi^a\phi^a)^2,$$

where the basic field ϕ^a is a $O(N)$ multiplet. In this letter, the conventional dimensional regularization is utilized for the ultra-violet divergences. Therefore, an extra factor $\Lambda^{2\varepsilon}$ is appended to the quartic interaction, where Λ is an arbitrary scale and $\varepsilon=2-D/2$. In the broken phase, we perform the following shift of the field variables

$$\phi^a=\pi^a \qquad a=1,2\cdots N-1, \tag{2}$$

$$\phi^N=v\Lambda^{-\varepsilon}+\sigma,$$

$$v^2=\frac{6\mu^2}{\lambda}=\frac{3m^2}{\lambda}.$$

After the shift, the Lagrangian looks like

$$L=L_0+L_{\text{int}}+\delta L, \tag{3}$$

$$L_0=\frac{1}{2}\partial_\mu\sigma\partial_\mu\sigma+\frac{m^2}{2}\sigma^2+\frac{1}{2}\partial_\mu\pi^a\partial_\mu\pi^a,$$

$$L_{\text{int}}=\frac{\lambda v\Lambda^{\varepsilon}}{3!}\sigma(\sigma^2+\pi^2)+\frac{\lambda\Lambda^{2\varepsilon}}{4!}(\sigma^2+\pi^2)^2,$$

$$\delta L=\left(\delta\mu^2+\frac{\delta\lambda}{6}v^2\right)v\Lambda^{-\varepsilon}\sigma+$$

$$\frac{\delta Z}{2}(\partial_\mu\sigma\partial_\mu\sigma+\partial_\mu\pi\partial_\mu\pi)+\left(\delta\mu^2+\frac{\delta\lambda}{2}v^2\right)\frac{\sigma^2}{2}+\left(\delta\mu^2+\frac{\delta\lambda}{6}v^2\right)\frac{\pi^2}{2}+$$

$$\frac{\delta\lambda v\Lambda^{\varepsilon}}{3!}\sigma(\sigma^2+\pi^2)+\frac{\delta\lambda\Lambda^{2\varepsilon}}{4!}(\sigma^2+\pi^2)^2 .$$

We now impose the following three mass-dependent renormalization conditions at some arbitrary scale κ[2,3]:

$$\delta v = 0 , \tag{4}$$

$$\Gamma^{\sigma\sigma}(p^2=\kappa^2) = Z(\kappa^2+m^2(\kappa^2)) ,$$

$$\frac{\mathrm{d}}{\mathrm{d}p^2}\Gamma^{\pi\pi}(p^2)|_{p^2=0} = 1 .$$

These conditions turn out to form a convenient choice of renormalization scheme. The first condition fixes the vacuum expectation value to its tree value hence eliminates all the tadpole diagrams. Due to the potential infra-red divergences for the σ correlation function at low-energies, the mass parameter of the σ particle is defined at some nonvanishing scale κ. This should render the theory both infra-red and ultra-violet finite. Through these renormalization conditions, the mass of the σ particle $m(\kappa)$ and the coupling constant $\lambda(\kappa)$ will depend on the scale κ. Of course, physics does not depend on the arbitrary scale κ-*a* fact that is represented by the renormalization group equations. The evolution equations for the mass of the σ particle and the renormalized coupling constants are determined by the renormalization group coefficients which could be calculated using perturbative loop expansion.

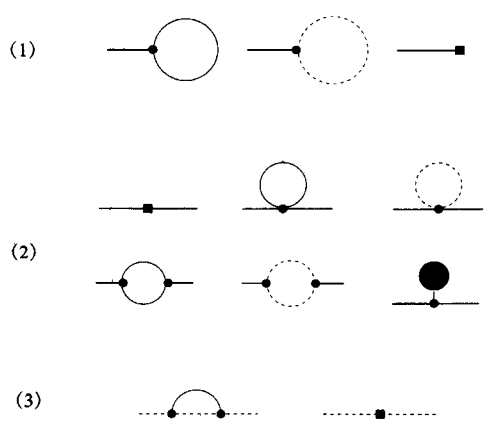

Fig. 1. The one-loop diagrams that enter the renormalization conditions (4) are listed. The solid lines represent σ propagators while the dotted lines designate Goldstone propagators. The black blob represents the vertex which arises from the counterterms with the number representing the order of the counterterm.

The calculation to one-loop is straightforward and the full mass-dependent renormalization group coefficients can be obtained. The corresponding Feynman diagrams are listed in Fig. 1. The renormalization group coefficients are defined by

$$\beta_\lambda = \kappa\frac{\mathrm{d}\lambda}{\mathrm{d}\kappa} , \tag{5}$$

$$\gamma_m = \frac{\kappa}{m^2}\frac{\mathrm{d}m^2}{\mathrm{d}\kappa} ,$$

where the derivatives are taken at fixed bare values. Using the fact that the bare quantities do not depend on the renormalization point κ, we obtain the following perturbative expansion for the renormalization group coefficients:

$$\frac{1}{\lambda}\beta_\lambda = -a_1'\lambda + (2c_1' - a_2' + 2a_1a_1' - 2c_1a_1')\lambda^2 , \tag{6}$$

$$\gamma_m = -b_1'\lambda + (c_2' - b_2' + b_1b_1' + b_1a_1' - c_1a_1')\lambda^2 ,$$

$$Z = 1 + c_1\lambda + c_2\lambda^2 + \cdots ,$$

$$\delta\lambda = a_1\lambda^2 + a_2\lambda^3 + \cdots ,$$

$$\delta\mu^2 = \mu^2(b_1\lambda + b_2\lambda^2 + \cdots) .$$

In the above equations the prime designates the derivative with respect to $\log\kappa$. Within the one-loop calculation, only coefficients a_1 and b_1 are needed. Therefore, we obtain the one-loop coefficients immediately,

$$\frac{1}{\lambda}\beta_\lambda = \gamma_m = \frac{3\lambda}{16\pi^2}\left[\int_0^1 \mathrm{d}x \frac{x(1-x)\,\kappa^2}{m^2 + x(1-x)\kappa^2} + \frac{N-1}{9}\right] . \tag{7}$$

Due to our first renormalization condition, the tree level relation $v^2 = 3m^2/\lambda$ remains valid at all scales and to all orders of perturbation theory. Therefore, the renormalization group coefficients for m^2 and λ are proportional to each other. Comparing with the conventional mass-independent beta-function of the theory, the mass-dependent betafunction exhibits different features as the scale κ is changed. At very low energies, i.e. $\kappa^2/m^2 \ll 1$, the first term in the beta-function is negligible and the beta-function is given by $(N-1)\lambda^2/(48\pi^2)$, which originates from the Goldstone loop contributions only. This shows that, at low energies, the renormalization effects are dominated by the Goldstones as expected. When the energy scale is increased, the first term which originates from the σ loop becomes significant. At high enough energies, the beta-function saturates to $(N+8)\lambda^2/(48\pi^2)$, which is the conventional result in a mass-independent renormalization scheme which treats the σ and the Goldstone particles equally. The low energy behavior can be extracted easily from the renormalization group flow of the above equations. As κ/m goes to zero, the running coupling constants λ goes to zero logarithmically as $(\log\kappa)^{-1}$. The correlation function $\Gamma^{\sigma\sigma}(\rho p)$ has the following asymptotic behavior,

$$\Gamma^{\sigma\sigma}(\rho p;\ \lambda,\ m^2,\ \kappa) \sim \frac{\lambda(\rho)v^2}{3}\left(1 - \frac{(N-1)\lambda(\rho)}{96\pi^2}\log\frac{\kappa^2}{p^2} + O(\lambda^2) + \cdots\right) . \tag{8}$$

Note that this agrees with the effective Lagrangian result for the Green's function,

$$G^{\sigma\sigma}(\rho p) \sim \log\rho + \text{constant} . \tag{9}$$

Therefore, at this stage we obtain the same result as in the effective Lagrangian approach[1,4]. However, there might be a potential problem. In the renormalization scheme that is used here, one can show[5] that the $\sigma\sigma$-correlation function always scales as λ. To one-loop level, the running coupling constant λ vanishes logarithmically which is a direct result from the evolution equation for λ in Eq. 7. However, if we were to include higher loop contributions in our calculation, the β-function will take the form:

$$\beta_\lambda = \beta_1\lambda^2 + \beta_2\lambda^3 + \cdots , \tag{10}$$

where the second term stems from the two-loop contributions. As a result, the evolution of the running coupling constant is modified to,

$$\lambda(\rho) \sim (\log\rho)^{-1} + \frac{\log\log\rho}{\log^2\rho} . \tag{11}$$

Therefore, the next to leading term in the $\sigma\sigma$-correlation function will generate a $\log\log\rho$ behavior. Within the context of the effective Lagrangian approach, however, the next to leading contribution only comes in as $\rho^2\log\rho$. It seems impossible to obtain a double logarithm behavior in the effective Lagrangian approach. The only way to reconcile this,

if one believes that both methods are valid, is that the coefficient β_2 has to vanish in the infrared limit. In the following, we will show, by explicitly calculating the two-loop beta-function in the infra-red limit, that this assertion is indeed true.

3 Two-loop renormalization group coefficients in the infra-red limit

In this section, the results of the two-loop RG coefficients in the infra-red limit will be given. The details of the calculation will be given elsewhere[5]. There are quite a number of diagrams at two-loop order. However, it can be shown that, in the infra-red limit only a few infra-red divergent diagrams contribute to the RG coefficients[5]. These diagrams are listed in Fig. 2. They fall into three categaories: bubbles, snails and diamonds.

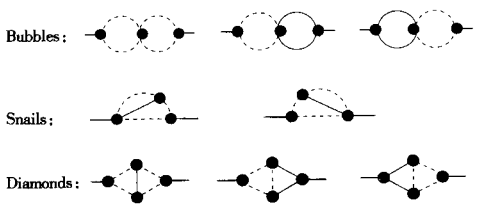

Fig.2. Two-loop diagrams that contribute to the renormalization group coefficients in the infra-red limit are listed. They fall into three categories: bubbles, snails and diamonds.

Bubble diagrams are just products of one-loop diagrams and can be obtained easily. In the infra-red limit, they contribute to the expansion coefficient a_2 in Eq. (6) as,

$$(a_2)_{\mathrm{B}} = -a_1^2 + \frac{N-1}{3} I_2(\kappa, m) I_3(\kappa) - \frac{N-1}{18} I_3^2(\kappa), \tag{12}$$

where the one-loop integrals are defined to be,

$$I_1(m^2) = \int \frac{\mathrm{d}^{2\omega} l}{(2\pi)^{2\omega}} \frac{\Lambda^{2\varepsilon}}{l^2 + m^2}, \tag{13}$$

$$I_2(\kappa, m) = \int \frac{\mathrm{d}^{2\omega} l}{(2\pi)^{2\omega}} \frac{\Lambda^{2\varepsilon}}{(l^2 + m^2)((l-\kappa)^2 + m^2)},$$

$$I_3(\kappa^2) = \int \frac{\mathrm{d}^{2\omega} l}{(2\pi)^{2\omega}} \frac{\Lambda^{2\varepsilon}}{l^2 (l-\kappa)^2}.$$

Using standard Feynman parametrization formula, one can write the snail diagrams as:

$$(a_2)_{\mathrm{S}} = -\frac{2N-2}{9} \left(\frac{\Lambda^2}{m^2}\right)^{2\varepsilon} \int \mathrm{d}x \int (l_1^2 + x(1-x)\kappa^2)^{-2} ((l_1 - l_2)^2 + 1)^{-1} l_2^{-2}, \tag{14}$$

where we have scaled out the mass. Note that we shifted l_1 integral but left the second factor untouched, since the change is only of the order κ^2/m^2 which is negligible in the infra-red limit. Performing the l_2 integral, we get,

$$(a_2)_{\mathrm{S}} = -\frac{2N-2}{9} \left(\frac{4\pi\Lambda^2}{m^2}\right)^{2\varepsilon} \frac{\Gamma(2\varepsilon)}{(4\pi)^4} \tag{15}$$

$$\int [y(1-y)]^{-\varepsilon} (1-\xi)^{-1+\varepsilon} \left(\xi x(1-x)\frac{\kappa^2}{m^2} + \frac{1-\xi}{1-y}\right)^{-2\varepsilon},$$

where we have replaced $\xi(1-\xi)^{-1+\varepsilon}$ by $(1-\xi)^{-1+\varepsilon}$ because the difference of the two only contributes an infra-red finite result which gives a vanishing contribution to the RG

coefficients in the infra-red limit. The integral can then be expressed in terms of the spence function and has the following limiting form:

$$(a_2)_S = \frac{2N-2}{9(4\pi)^4}\int\left(\frac{1}{\varepsilon}+2\psi(1)+2\log\frac{4\pi\Lambda^2}{m^2}\right)\log\frac{\kappa^2}{m^2}-\frac{1}{2}\log^2\left(x(1-x)(1-y)\frac{\kappa^2}{m^2}\right). \quad (16)$$

Finally let us calculate the diamond diagrams. They are UV finite but may contain infra-red divergences. Adding up the results from all the infra-red divergent diamonds, we have,

$$(a_2)_D = \frac{N-1}{18(4\pi)^4}\int\log\left(x(1-x)\frac{e\kappa^2}{m^2}\right)\log\left(y(1-y)\frac{\kappa^2}{m^2}\right)-5\log\left(x(1-x)(1-\xi)\frac{\kappa^2}{m^2}\right). \quad (17)$$

Now let us summarize the above calculation by adding up the results from Eq. (12), Eq. (16) and Eq. (17). We see clearly the derivatives of order λ^3 cancels out exactly and we obtain the same result as in the one-loop result. Also the $\sigma\sigma$ correlation function adds up to a geometric series,

$$\frac{1}{\lambda}\beta_\lambda = \frac{3\lambda}{16\pi^2}\left(\frac{N-1}{9}\right), \quad (18)$$

$$\Gamma^{\sigma\sigma}(p^2) = \frac{\lambda v^2}{3}\left(1-\frac{N-1}{6}\frac{\lambda}{16\pi^2}\log\frac{\kappa^2}{p^2}+\left(\frac{N-1}{6}\right)^2\left(\frac{\lambda}{16\pi^2}\right)^2\log^2\frac{\kappa^2}{m^2}\right).$$

The Greens function coincides with the result in the effective Lagrangian approach. This means that higher loops do not generate new infra-red divergences into the theory. The only infra-red divergence stems from the one-loop order and chiral symmetry guarantees that all the infra-red divergences cancel out in higher loops.

4 Conclusion

In this letter, the renormalization group properties of the $O(N)$ model in the broken phase is studied within the framework of field theory using perturbation theory. A mass-dependent renormalization scheme is used to handle the potential infra-red divergences in the theory in 4 dimensions. The corresponding renormalization group coefficients are obtained to oneloop at all scales and to two-loop in the infra-red limit. It is seen, by explicit perturbative calculation, that the two-loop renormalization group coefficients coincide with the one-loop result in the infra-red limit. As a result, the $\sigma\sigma$ Green's function agrees with the expected result obtained within the effective Lagrangian approach. The result also suggests, that the potential infra-red divergences in the theory is in fact only a one-loop effect.

The author would like to thank J. Kuti and A. Manohar for helpful discussions.

References

1 Gasser J, Leutwyler H. Phys. Lett., 1983, **125B**:321,325; Ann. of Phys., 1984, **158**:142; Nucl. Phys., 1985, **B250**:465
2 Kuti J. Nucl. Phys., 1995, **B**(Proc. Suppl.) **42**:113
3 Liu C, Jansen K, Kuti J. Nucl. Phys., 1995, **B**(Proc. Suppl.) **42**:630
4 Gasser J, Leutwyler H. Nucl. Phys., 1988, **B307**:763
5 Kuti J, Liu C. unpublished.

$O(N)$模型破缺相的红外重正化群计算

刘 川

(北京大学物理系 北京 100871)

摘要 利用一个与质量有关的重正化方案,研究了$O(N)$模型破缺相的红外重正化群性质. 得到了与质量有关的一圈重正化群系数以及在红外极限下的二圈重正化群系数. 利用标准的微扰场论计算方法,发现特殊的抵消效应,该效应使得二圈的重正化群系数与一圈重正化群系数在红外极限下相同.

关键词 红外重正化群 有效拉氏量 $O(N)$模型 破缺对称性

1999-01-04收稿